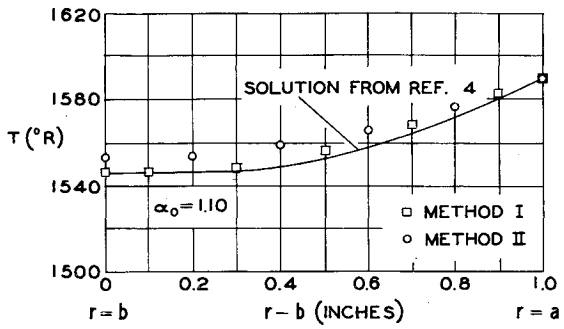

Fig. 1 Temperature profiles at melt time ($t = t_m$).

will always be linear in the highest order derivative term (when more than three terms are used in the expansion).

The series expansion of the temperature is terminated after $2K$ or $2K + 1$ terms, thus leading to a differential equation of Kth order. Thus, in addition to the initial conditions $R_s(0) = 0$, and $\dot{R}_s(0) = 0$, it is required to obtain K − 2 additional conditions. These $K - 2$ values, $\ddot{R}_s(0)$, $\dddot{R}_s(0)$ . . ., are obtained by matching the initial temperature distribution $\theta_0(Z, 0)$ at $K - 2$ points.

Method 2

An investigation of the heat balance integral technique for slabs is discussed by Goodman.[2] Basically, the technique is much the same as the momentum integral of fluid dynamics. The heat-conduction equation is satisfied on the average and a temperature profile is assumed. In the problem considered here, a second-degree polynomial temperature profile is assumed, and the three arbitrary constants are evaluated from the boundary conditions.

The substitution of the assumed temperature profile

$$T = T_m - \left[\frac{Q + \rho L(dr_s/dt)}{2k}\right]\left[(r_s - b) - \frac{(r - b)^2}{(r_s - b)}\right] \qquad r_s \neq b \quad (7)$$

into the integrated heat-conduction equation (1) yields the following second order, nonlinear, ordinary differential equation for $r_s(t)$:

$$\frac{d^2r_s}{dt^2} = -\left[\frac{Q}{\rho L} + \frac{dr_s}{dt}\right] \times \left\{\frac{(r_s - b)(9r_s + 7b)(dr_s/dt) + 12\kappa(3r_s - b)}{(r_s - b)^2(3r_s + 5b)}\right\} \quad (8)$$

It should be noted that Eq. (8) is applicable for temperature-independent material properties only. For materials with temperature-dependent properties, a similar procedure leads to an integrodifferential equation.

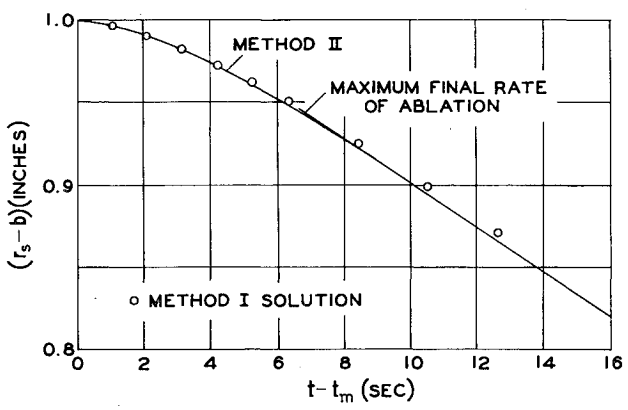

Fig. 2 Ablation depth vs time for $\alpha_0 = 1.10$.

Discussion

Numerical calculations using both methods 1 and 2 have been performed for a 1-in. thick $7\frac{3}{4}$-in. o.d. aluminum sphere subjected to a constant radial heat flux.‡ Average constant thermal and physical properties were assumed.[5] The analysis was performed for a value of $\alpha_0 = 1.10$ (where α_0 is the nondimensional surface heat-transfer coefficient ha/k) and a stagnation temperature of 1850°R.

The premelt solution for the temperature was obtained through the use of existing solutions.[4] In order to approximate the temperature profile at the melt time with sufficient accuracy, a six-term Taylor series expansion was used in method 1 (from which the required initial conditions on R_s were obtained). A comparison of the calculated temperature profile at melt time indicates that the assumed quadratic profile used in method 2 is in good agreement with both the exact premelt solution and the solution obtained from method 1 (Fig. 1).

The melt depth predicted by both methods is in excellent agreement (Fig. 2). Furthermore, as shown in Fig. 2, the rate of ablation rapidly approaches a constant value.

In conclusion, it is clearly seen that the numerically simpler technique (method 2) can be applied to the ablating sphere and yields results that are quite close to those obtained using the more complex technique (method 1). Both of these methods predict ablation profiles that are almost identical.

References

[1] Citron, S. J., "On the conduction of heat in a melting slab," Columbia Univ., Dept. of Civil Engineering and Engineering Mechanics TR 18 (March 1961).

[2] Goodman, T. R., "The heat balance integral and its application to problems involving a change of phase," Trans. Am. Soc. Mech. Engrs. **80**, 335–342 (February 1958).

[3] Carslaw, H. S. and Jaeger, J. C., *Conduction of Heat in Solids* (Clarendon Press, Oxford, England, 1959), 2nd ed., pp. 126, 230.

[4] Smithson, R. E. and Thorne, C. J., "Temperature tables," U. S. Naval Ordnance Test Station, NAVORD Rept. 5562, Part 6, NOTS 2088 (September 1958).

[5] Parisse, R. F. and Klosner, J. M., "Ablation of a hollow sphere," Polytechnic Institute of Brooklyn, PIBAL Rept. 670 (August 1963).

‡ Since the surface temperature is assumed to remain at the melt temperature during the melt analysis, a constant heat flux corresponds to steady-state aerodynamic heating during melting.

Bow Shock Shape About a Spherical Nose

RICHARD J. BERMAN*
General Electric Company, King of Prussia, Pa.

Nomenclature

e_s	=	eccentricity factor, Eq. (1)
M	=	Mach number
R_N	=	body nose radius
R_s	=	nose radius of bow shock wave
r_s	=	lateral coordinate of the bow shock wave
X	=	body axial distance measured from the body nose
X'	=	axial distance measured from shock apex
Δ	=	stagnation-point shock standoff distance
ρ_∞/ρ_2	=	density ratio across a normal shock

Received November 18, 1964.

* Engineer, Aerodynamics Advanced Design and Analysis, Missile and Space Division. Member AIAA.

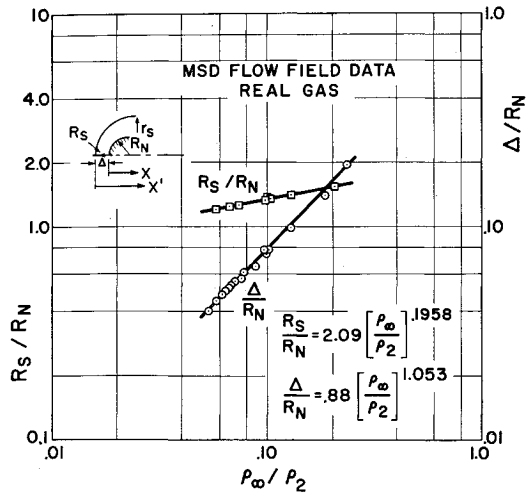

Fig. 1 Correlation of shock-to-body radius ratio and shock standoff distance with density ratio.

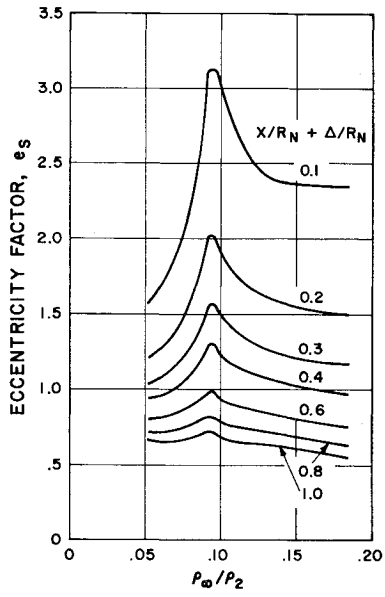

Fig. 3 Shock-shape eccentricity factor.

Introduction

METHODS for predicting the bow shock-wave shape for blunt bodies such as sphere cones have been developed previously.[1] For purposes of predicting the over-all shock-layer thickness or the location of control surface-bow shock interaction, these available methods are adequate. However, for the purpose of determining bow shock-wave-generated vorticity necessary in the analysis of entropy gradient effects on skin friction and heat transfer, these methods, which have their basis in blast-wave theory, are inadequate. This is especially so in the vicinity of the nose, the very place where the greatest degree of shock-layer vorticity is introduced into the flow field.

Therefore, the purpose of this note is to present a simplified method to predict the bow shock-wave shape about a spherical nose for an inviscid gas, which is in chemical equilibrium at Mach numbers greater than 5.0. This method is based on a correlation of data obtained from exact numerical General Electric flow-field calculations and is intended to be applied in the region from the shock apex to a station approximately one nose radius downstream.

Discussion and Results

In order to obtain a relatively simple but accurate method for predicting the bow shock shape, an attempt was made to correlate available General Electric flow-field results. The relation selected initially to obtain this correlation was the equation for conic sections utilized by Van Dyke and Gordon in Ref. 2; that is,

$$r_s^2 = 2R_sX' - e_sX'^2 \tag{1}$$

To facilitate the use of Eq. (1), the origin of the coordinates is translated to the nose of the body by substituting $X' = X + \Delta$. Then normalizing by the body nose radius R_N yields

$$\left(\frac{r_s}{R_N}\right)^2 = 2\left(\frac{R_s}{R_N}\right)\left(\frac{X}{R_N} + \frac{\Delta}{R_N}\right) - e_s\left(\frac{X}{R_N} + \frac{\Delta}{R_N}\right)^2 \tag{2}$$

The shock standoff distance Δ was obtained from a correlation of values available from General Electric flow-field solutions.[3] This correlation (Fig. 1) is obtained by use of the density ratio across a normal shock ρ_∞/ρ_2 as suggested in Refs. 2–5.

Because of its applicability to the correlation of Δ, the density ratio is also used in this study to correlate the ratio of the radius of curvature of the shock and the body (R_s/R_N) measured at the axis. Summary plots of these radius ratio parameters obtained from the flow-field data are also pre-

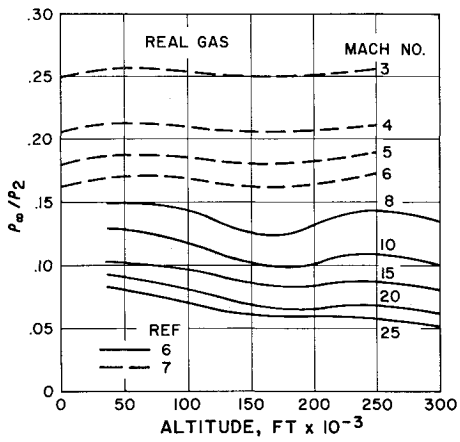

Fig. 2 Density ratio across normal shock.

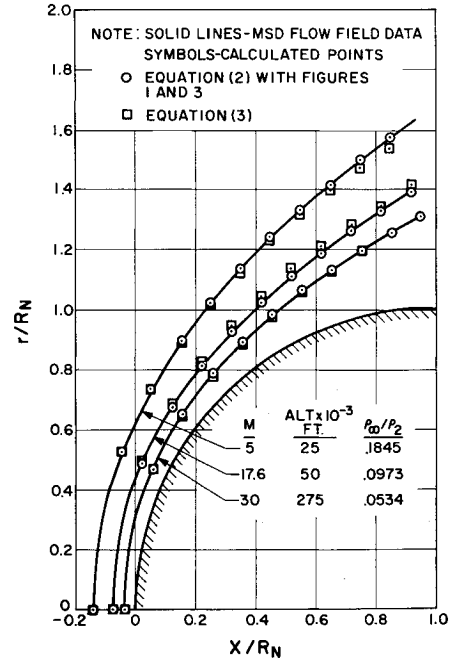

Fig. 4 Comparison of bow shock shapes.

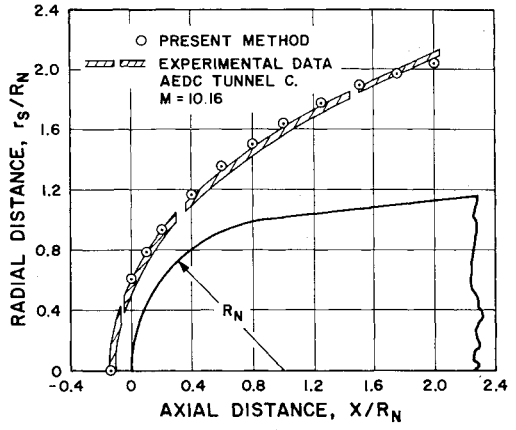

Fig. 5 Comparison of theoretical and experimental shock shape, nose region.

sented in Fig. 1. In order to facilitate the use of these correlations for specific flight conditions, the density ratio parameters calculated for various Mach number and altitude combinations are presented in Fig. 2. This plot is for an inviscid gas at chemical equilibrium.[6,7]

By use of flow-field data, Eq. (2) has been solved for the eccentricity factor e_s. These results (shown in Fig. 3) indicate a dependence upon the density ratio as expected; however, a dependence upon the axial distance is also indicated. It is further noted that, for any given axial station, e_s is nonlinear with density ratio and peaks at approximately $\rho_\infty/\rho_2 = 0.095$.

Equation (2) may now be solved for almost any combination of Mach number and altitude of interest ($0.05 \leq \rho_\infty/\rho_2 \leq 0.25$) to obtain r_s as a function of X. Figures 1–3 provide all of the necessary data.

The results of the application of this method are presented in Fig. 4 for several freestream conditions and are compared with General Electric Missile and Space Division flow-field data. Figure 5 presents theoretical and experimental shock-shape data. These comparisons indicate excellent agreement between the correlation method [Eq. (2) with Figs. 1–3] and the exact flow-field data.

Approximate Method

A more approximate solution for the bow shock wave has also been obtained by approximating the eccentricity data in Fig. 3 with a single analytical expression, determining relations for the curves in Fig. 1 and incorporating these expressions into Eq. (2). This approximate solution may be expressed by the single equation

$$\frac{r_s}{R_N} = \left\{4.18\left(\frac{\rho_\infty}{\rho_2}\right)^{0.1958}\left[\frac{X}{R_N} + 0.880\left(\frac{\rho_\infty}{\rho_2}\right)^{1.053}\right] - 0.646\left[\frac{X}{R_N} + 0.880\left(\frac{\rho_\infty}{\rho_2}\right)^{1.053}\right]^{1.467}\right\}^{0.5} \quad (3)$$

The results of the application of this approximate relation [Eq. (3)] are also presented in Fig. 4 where relatively good agreement is indicated.

References

[1] Berman, R. J., "A method for the prediction of the bow shock wave about sphere-cone configurations," General Electric Missile and Space Vehicle Div., Rept. AFM 127 (August 1961).

[2] Van Dyke, M. D. and Gordon, H. D., "Supersonic flow past a family of blunt axisymmetric bodies," NASA TR R-1 (1959).

[3] Ridyard, H. W. and Storer, E. M., "Stagnation-point shock detachment of blunt bodies in supersonic flow," J. Aerospace Sci. **29**, 751–752 (1962).

[4] Serbin, H., "Supersonic flow around blunt bodies," J. Aerospace Sci. **25**, 58–59 (1958).

[5] Li, T.-Y. and Geiger, R. E., "Stagnation point of a blunt body in hypersonic flow," J. Aerospace Sci. **24**, 25–32 (1957).

[6] Huber, P. W., "Tables and graphs of normal-shock parameters at hypersonic Mach numbers and selected altitudes," NACA TN 4352 (1958).

[7] "Normal and oblique shock characteristics at hypersonic speeds," Douglas Aircraft, Engineering Rept. LB-25599 suppl. I (1959).

Natural Frequencies of Orthotropic Circular Plates

K. A. V. Pandalai* and Sharad A. Patel†
Madras Institute of Technology, Madras, India

THIS note is concerned with the determination of natural frequencies of orthotropic circular plates. A circular plate fabricated with radial and/or circumferential reinforcements may be idealized as an orthotropic plate of uniform thickness with different material properties in the radial and circumferential directions. The stress-strain relations for such plates can be written in a manner analogous to that given in Ref. 1:

$$\begin{aligned} \sigma_r &= E_1\epsilon_r + E_{12}\epsilon_\theta \\ \sigma_\theta &= E_2\epsilon_\theta + E_{12}\epsilon_r \\ \tau_{r\theta} &= G\gamma_{r\theta} \end{aligned} \quad (1)$$

where E_1, E_{12}, E_2, and G are material constants. With the usual assumptions of small-deflection theory of plates, the following relations between moments and the lateral deflection $W(r,\theta)$ of the plate are obtained:

$$\begin{aligned} M_r &= -D_r\left[\frac{\partial^2 W}{\partial r^2} + \alpha\left(\frac{1}{r}\frac{\partial W}{\partial r} + \frac{1}{r^2}\frac{\partial^2 W}{\partial \theta^2}\right)\right] \\ M_\theta &= -D_r\left[\beta\left(\frac{1}{r}\frac{\partial W}{\partial r} + \frac{1}{r^2}\frac{\partial^2 W}{\partial \theta^2}\right) + \alpha\frac{\partial^2 W}{\partial r^2}\right] \\ M_{r\theta} &= -2\gamma D_r\frac{\partial}{\partial r}\left[\frac{1}{r}\frac{\partial W}{\partial \theta}\right] \end{aligned} \quad (2)$$

In the foregoing, $D_r = E_1h^3/12$, $\alpha = E_{12}/E_1$, $\beta = E_2/E_1$, and $\gamma = G/E_1$. Also, h is the thickness of the plate. The governing equilibrium equation for the plate in terms of these moments is

$$\frac{\partial^2}{\partial r^2}(rM_r) + \frac{2}{r}\frac{\partial}{\partial r}\left(r\frac{\partial M_{r\theta}}{\partial \theta}\right) - \frac{\partial M_\theta}{\partial r} + \frac{1}{r}\frac{\partial^2 M_\theta}{\partial \theta^2} = -rq(r,\theta) \quad (3)$$

where $q(r,\theta)$ is the load intensity. For a free vibration problem, $q = -\rho(\partial^2 W/\partial t^2)$, where $W = W(r,\theta,t)$ and ρ is mass per unit area of the plate. Substitution of Eq. (2) into Eq. (3) yields the governing equation for the free vibration of the plate as

$$r\frac{\partial^4 W}{\partial r^4} + 2\frac{\partial^2 W}{\partial r^3} - \beta\left(\frac{1}{r}\frac{\partial^2 W}{\partial r^2} - \frac{1}{r^2}\frac{\partial W}{\partial r}\right) + \frac{\beta}{r^3}\left(\frac{\partial^4 W}{\partial \theta^4} + 2\frac{\partial^2 W}{\partial \theta^2}\right) + 2(\alpha + 2\gamma) \times \frac{\partial^2}{\partial \theta^2}\left(\frac{1}{r}\frac{\partial^2 W}{\partial r^2} - \frac{1}{r^2}\frac{\partial W}{\partial r} + \frac{1}{r^3}W\right) = -\rho r\frac{\partial^2 W}{\partial t^2} \quad (4)$$

Received December 28, 1964.

* Professor and Head, Department of Aeronautical Engineering.

† Visiting Professor from Polytechnic Institute of Brooklyn, Brooklyn, N. York. Associate Fellow Member AIAA.